A New Approach to the Study of Amine-CO_2 System Based on the Absolute Reaction Rate Theory

Toru Yamaguchi*[1], Hidetaka Yamada[2], Syohei Sanada[1] and Kenji Hori[1,3]

[1] Division of Computational Chemistry, Transition State Technology Co. Ltd.
2-16-1 Tokiwadai, Ube, Yamaguchi 755-8611, Japan
[2] Frontier Science and Social Co-creation Initiative, Kanazawa University
Kakuma-machi, Kanazawa, Ishikawa 920-1192, Japan
[3] Graduate School of Sciences and Technology for Innovation, Yamaguchi University
2-16-1 Tokiwadai, Ube, Yamaguchi 755-8611, Japan

E-mail : tor@tstcl.jp Tel : +81-836-35-9228 FAX : +81-836-35-9228

Abstract

For understanding the reaction and controlling its process, it is very important to clarify the reaction profile such as time evolution of substrates in the solution. In this respect, we have developed a reaction kinetics simulator; Kinerator. This program simulates the rate of reaction progress using those free energies. However, in case of solving a complicated system in which the reaction rates are significantly different and some reactions sharing same substrates exist, there is a problem that the computational time to carry on numerical integration becomes huge. In our recent studies, we reviewed the reaction kinetics, devised the simultaneous ordinary differential equation to efficiently solve these complicated systems using numerical solutions and implemented it to our Kinerator. In this study, we applied the simulator to AMP(2-amino-2-methyl-1-propanol) –CO_2 system due to clarify the detailed reaction profiles in a short time range depending on CO_2 concentrations. We were able to reproduce actual measurement values with extremely high accuracy using free energies obtained by quantum chemical calculations at SMD/B3LYP/6-311++G(d,p)//SMD/B3LYP/6-31G(d) level of theory.

Keywords

Reaction Kinetics, Kinerator, CO_2 absorption

1. Introduction

Tracking the time evolution in concentrations of reactants and products in the reaction solvent is very important for understanding the reaction and controlling the process. Although

actual reactions are complicated systems having multiple reactions with different types and kinetics, we consider that computer simulations can reproduce their concentration changes if we could feed rate constants of each reactions and the relationship of substances between multiple reactions. Quantum chemical calculations can predict energy diagrams for these reactions including their transition states, which characterizes the details of reaction mechanisms and their thermodynamics. The methodology to obtain reaction rate constants theoretically from the predicted energies is formulated as the absolute reaction rate theory [1-3] by Eyring and Polanyi, and systemize as a transition state theory by Laidler and King [4-5]. The transition state theory defines reaction rate as the frequency of passing through transition states. Therefore, if we can identify the three points of the reactant, transition state and product by reaction analysis with accurate activation free energy, we can apply calculated results to the Eyring-Polanyi equation due to track the time evolution in concentrations of substances correctly. For this purpose, we have been developing a reaction kinetics simulator; Kinerator [6] which can simulate the rate of reaction progress using calculated free energies.

There are several algorithms to solve the Eyring-Polanyi equation. In Kinerator, the normal numerical integration and MSE (Multi-Step Equilibrating) algorithm [6] are implemented. However, in case of solving a complicated system in which the reaction rates are significantly different and some reactions sharing same substrates exist, there is a problem that the computational time to carry on numerical integration becomes huge. In our recent studies, we reviewed the Eyring-Polanyi equation and devised the simultaneous ordinary differential equation to efficiently solve these complicated systems using numerical solutions. We implemented the equation to our Kinerator and applied some systems due to confirm the results. In this study, we applied this algorithm and the simulator to the AMP(2-amino-2-methyl-1-propanol)-CO_2 system and clarify detailed reaction profiles in a short time range depending on CO_2 concentratios. We were able to reproduce actual measurement values [7] with extremely high accuracy using free energies obtained by SMD/B3LYP/6-311++G(d,p)//SMD/B3LYP/6-31G(d) level of theory based on the proposed mechanism of Yamada *et al.* [8].

2. Computational Details

2.1. Reaction Kinetics

The reaction rate can be theoretically defined by Eq. (1). According to this equation, the rate constant k in the reaction can be represented by the product of the equilibrium constant $K^{\ddagger}$, which represents the ratio of the transition state to the substance at the equilibrium state, υ and κ. υ is the value obtained by dividing the product of the Boltzmann constant k_B and reaction temperature T by the Planck's constant h, which is shown in Eq. (2). This value indicates the frequency with which the reaction passes through the transition state. κ is called

the transmission coefficient from 0 to 1 which is a correction related to factors that hinder the reaction represented by the reverse reaction progress, tunneling effects and others.

$$k = \kappa \cdot \upsilon \cdot K^{\ddagger} \quad (1)$$

$$\upsilon = \frac{k_B T}{h} \quad (2)$$

Assuming that κ depends only on the reverse reaction progress, with dividing $K^{\ddagger}$ to the forward and reverse reaction, it can be written as Eq. (3).

$$k = \upsilon \cdot \left(K_1^{\ddagger} - K_{-1}^{\ddagger}\right) \quad (3)$$

where $K_1^{\ddagger}$ indicates the equilibrium constant of the forward reaction and $K_{-1}^{\ddagger}$ is of the reverse reaction. In the absolute rate theory, the forward equilibrium constant $K_1^{\ddagger}$ can be represented as Eq. (4) using the activation free energy $\Delta G^{\ddagger\circ}$ under standard condition, where R is the gas constant.

$$K_1^{\ddagger} = exp\left(-\frac{\Delta G^{\ddagger\circ}}{RT}\right) \quad (4)$$

The $\Delta G^{\ddagger\circ}$ can be obtained from quantum chemical calculations along IRC. They either can derive the reaction free energy ΔG_{rxn}°. Plugging ΔG_{rxn}° into Eq. (5) leads the reverse equilibrium constant $K_{-1}^{\ddagger}$, and then k can be found.

$$K_{-1}^{\ddagger} = exp\left(-\frac{(\Delta G^{\ddagger\circ} - \Delta G_{rxn}^{\circ})}{RT}\right) \quad (5)$$

Considering a reaction consuming substrate A, this consumption rate can be expressed by Eq. (6) using the reaction rate constant. Here, dt represents a minute difference of time.

$$-\frac{d[A]}{dt} = k[A] \quad (6)$$

Integrating Eq. (6) with respect to substrate A by Eq. (7) and (8), the substrate concentration at a certain reaction time t can be obtained. $[A]_0$ is the initial concentration of the substrate.

$$\int_{[A]_0}^{[A]_t} \frac{d[A]}{[A]} = -k \int_0^t dt \quad (7)$$

$$[A]_t = [A]_0 \cdot exp(-k \cdot t) \quad (8)$$

When the substrate is involved in n multiple reactions in the same system, it can be written as Eq. (9) using the rate constant k^i of each reaction i. Z is the sign of 1 or -1. $Z = 1$ is for the consumption of the substance and $Z = -1$ is for the production.

$$\sum_i^n \int_{[R]_0}^{[R]_t} \frac{d[R]}{[R]} dt = \sum_i^n Z \cdot k^i \int_0^t dt \quad (9)$$

By setting Eq. (9) for all the substrates in the system and solving them simultaneously, it will be possible to obtain the concentration change of each substrate with time. However, this equation cannot be solved analytically, and numerical integration must be performed. In addition, it is necessary to take dt as enough small as possible for the reaction in the time integration. In the case that the rate of a target reaction is fast, the computational cost for the

numerical integration becomes enormous in association with a long time simulation. Therefore, using Eq. (9), it is not practical to solve a complicated system in which multiple reactions with different time scales sharing substrates are mixed.

For the general system, when reactions $i = 1,2,3,\ldots$ expressed by Eq. (10) including substrates $I = A, B, C, \ldots$ present in the same system,

$$n_i^A A + n_i^B B + \cdots + n_i^I I \underset{k_{-i}}{\overset{k_i}{\rightleftarrows}} \cdots + m_i^C C + m_i^D D + \cdots + m_i^I I \quad (10)$$

it is considered that the unit reduction amount x_i of the reaction i can be expressed by Eq. (11) using the product of the rate constant and concentration of each substrate, where $cmps$ means all substrates.

$$\frac{dx_i}{dt} = k_i \prod_{I=A,B,C,\ldots}^{cmps} [I]^{n_i^I} - k_{-i} \prod_{I=A,B,C,\ldots}^{cmps} [I]^{m_i^I} \quad (11)$$

Here, the concentration of substrate I is derived from Eq. (12) as the difference between the initial concentration of I and X_I the reduction amount of I.

$$[I] = [I]_0 - X_I \quad (12)$$

X_I can be calculated by Eq. (13) by adding the unit reduction and production amount of each reaction i including the reaction I. Here, $rxns$ means all reactions.

$$X_I = \sum_{i=1,2,3,\ldots}^{rxns} n_i^I \cdot x_i - \sum_{i=1,2,3,\ldots}^{rxns} m_i^I \cdot x_i \quad (13)$$

Since Eq. (11) is a function of x_i of each reaction, with setting this like Eq. (14), all reactions containing in the same system can be expressed by Eq. (15).

$$\frac{dx_i}{dt} = F_i(x_1, x_2, \cdots, x_i, \cdots) \quad (14)$$

$$\begin{pmatrix} dx_1 \\ dx_2 \\ \vdots \\ dx_i \\ \vdots \end{pmatrix} = \begin{pmatrix} F_1(x_1, x_2, \cdots, x_i, \cdots) \\ F_2(x_1, x_2, \cdots, x_i, \cdots) \\ \vdots \\ F_i(x_1, x_2, \cdots, x_i, \cdots) \\ \vdots \end{pmatrix} dt \quad (15)$$

If we can solve this simultaneous ordinary differential equation Eq. (15), the unit reduction amount x_i at time t of each reaction can be obtained. As a result, the concentration of each substrate at a certain time can be calculated. At this time, we can set dt arbitrarily regardless of the reaction rate of each reaction, so this formula can be applied to complicated systems in which reactions having different time scales coexist. Moreover, since the whole reaction can be handled as a set, calculation is possible even when substrates are shared by multiple reactions. Therefore, by applying this formula to reaction analysis results by quantum chemical

calculations, it is possible to accurately calculate the difference of velocity of each reaction including reverse reactions, the reaction profile changes, half-life time of reactants, time to reaction equilibration, final production ratio, temperature dependence of reaction time and production ratio and etc. in a very fine time range without any measured values.

2.2. Reaction Analysis

The amine solution absorbing reaction of CO_2 is a well-known acid-base reaction, however it is a complicated system in which multiple pathways yield various intermediates and products. Yamada *et al.* [8] investigated the reactions and found activation energies of reactions 1 to 5 shown in Table 1 for AMP (2-amino-2-methyl-1-propanol) with optimizing transition states by B3LYP/6-31G(d) level of density functional theory calculations applied SCRF/IEF-PCM method with SMD model [9] in aqueous solution. In terms of this analysis, we performed structure optimizations and vibration analyses due to obtain free energies of these reactions. The calculations were carried out at the SMD/B3LYP/6-311++G(d, p) level of theory using the structures of Yamada *et al.* as initial structures. The vibration analyses were performed in the standard condition of 298.15K and 1atm, and it was confirmed that transition states have only one imaginary frequency. Gaussian09 [10] program was used for all calculations.

3. Results and discussions

For the AMP-CO_2 system, we obtained activation and reaction free energies shown together in Table 1. Figure 1 shows the energy diagram of these reactions with optimized transition state structures. Theoretical results shows that CO_2 absorption by AMP in an aqueous solution proceeds with 5 elementary routes having TS1 to 5. It is unlikely that a zwitterion exists in the gas phase because of its unstable structure. However, the reaction free energy ΔG_{rxn} of the zwitterion $RNH_2^+COO^-$ was calculated as -4.6 kcal mol^{-1}. It suggests the zwitterion can exist as an intermediate in the aqueous solution. The most stable point in this system is HCO_3^- + RNH_3^+ with ΔG_{rxn} = -11.3 kcal mol^{-1}. Therefore, CO_2 must transform to bicarbonate form. Alternatively, the carbamate form $RNHCOO^-$ + RNH_2^+ is also stable relatively with ΔG_{rxn} = -10.7 kcal mol^{-1}, so this formation is also possible. Since $\Delta G^‡$ of TS1 to 4 is 18.4 kcal mol^{-1} or less, routes of TS1 to 4 can proceed at room temperature. In contrast, $\Delta G^‡$ of TS5 is as high as 39.0 kcal mol^{-1}. Thus, there is the low possibility of bicarbonate production by this route.

Table 1

Results of AMP at SMD/B3LYP/6-311++G(d,p)//SMD/B3LYP/6-31G(d) level of theory.

TS	reactants	products	activation energies E_a [kcal mol^{-1}][a]		Gibbs free activation energies $\Delta G^{\ddagger}$ [kcal mol^{-1}][b]	
			forward	inverse	forward	inverse
1	$RNH_2^+COO^- + H_2O$	$RNHCOOH + H_2O$	20.1	22.9	18.4	19.2
2	$RNH_2 + CO_2$	$RNH_2^+COO^-$	4.1	6.4	3.5	8.1
3	$RNH_2^+COO^- + RNH_2$	$RNHCOO^- + RNH_3^+$	1.6	8.7	-0.8	5.3
4	$RNH_2 + CO_2 + H_2O$	$HCO_3^- + RNH_3^+$	9.0	16.8	6.6	18.0
5	$RNHCOO^- + H_2O$	$HCO_3^- + RNH_2$	40.0	41.7	39.0	32.7

[a]values obtained by Yamada *et al.* . [b]our values computed by vibrational analyses with SMD/B3LYP/6-311++G(d,p)//SMD /B3LYP/6-31G(d) level of theory in aqueous solution.

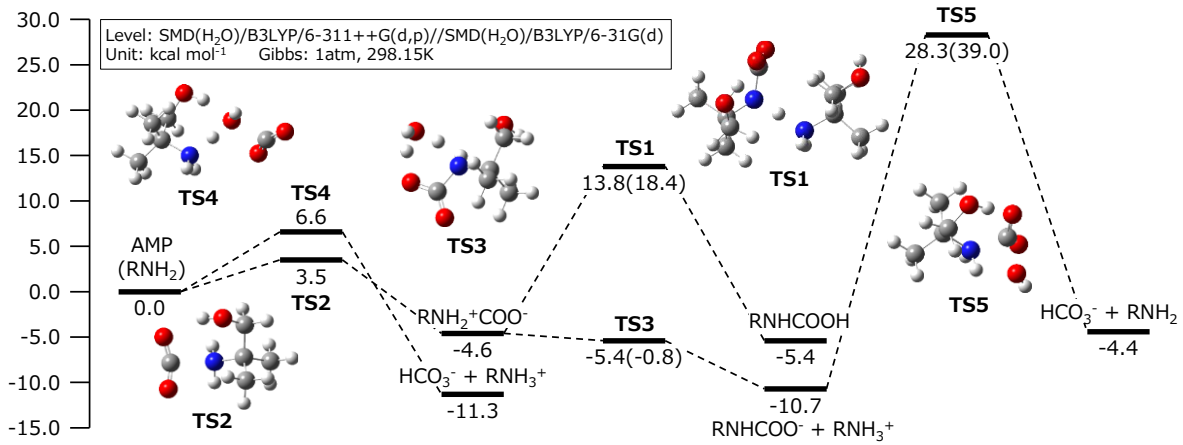

Figure 1 Energy diagram of AMP CO_2 absorption reaction at SMD/B3LYP/6-311++G(d,p)// SMD/B3LYP/6-31G(d) level of theory.

For these reactions, in order to clarify the reaction profile change due to differences in initial CO_2 concentrations, we performed kinetic simulations. The forward and inverse activation free energies $\Delta G^{\ddagger}$ shown in Table 1 were inputted to Kinerator and simulations were carried out from α the CO_2 loading ratio to AMP is 0.05 to 0.95 at 25 °C. In these simulations, the initial concentration ratio of each substrate $[AMP]_0 : [CO_2]_0 : [H_2O]_0$ is set to 1.0 : 0.05 – 0.95 : 12.0 in order to reproduce the general AMP solution of 30 wt% for using as an absorber of CO_2. Figure 2 shows the simulation result at α = 0.95 at 25 °C. The horizontal axis of the graph is the reaction time on a logarithmic scale, and the vertical axis is the value of mass molar concentration (mol/kg・H_2O) of substrates in a 30 wt% AMP solution. At the initial stage of the reaction of t = 1×10^{-11} to 1×10^{-10}, twice the amount of AMP as CO_2 is consumed quickly to produce RNH_3^+ and $RNHCOO^-$ carbamate ions. After t = 1×10^{-10}, its absorption rate slows down and we can observe the production and consumption of the zwitterion $RNH_2^+COO^-$. The

rate recovers at the latter half after t = 1×10^{-6} and the ratio of bicarbonate HCO_3^- increases as the last product of this absorption.

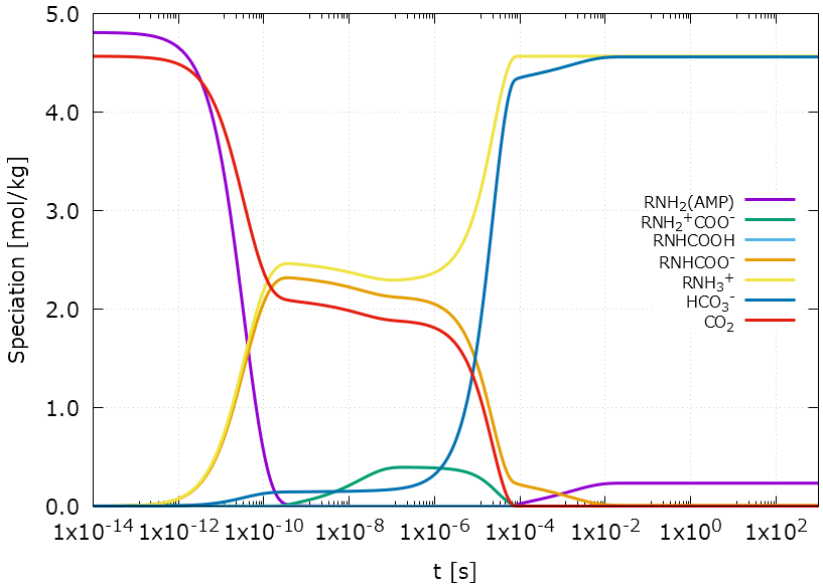

Figure 2 Simulated reaction profile at 25 °C.

While AMP can be consumed in an amount twice as much as CO_2 at the early stage of the reaction, it reaches saturation at α = 0.50. In response to the saturation, it was confirmed that $RNH_2^+COO^-$ was produced and disappeared at t = 1×10^{-10} to 10^{-4}. According to the energy diagram of Figure 1, it seems that this zwitterion does not have a stable point so that it seems impossible to be observed experimentally. On the other hand, we consider that our simulation results represented in Figure 2 suggest that it can be possible to detect the zwitterion with very microscopic observations when the CO_2 concentration is relatively high compared to AMP. In addition, the formation of $RNH_2^+COO^-$ and the rapid increase of HCO_3^- around t = 1×10^{-6} to 10^{-4} are solid proof that carbamates changes to bicarbonates through the reverse route via TS3 and TS4. Therefore, we think that our simulation theoretically indicates that produced HCO_3^- in this system is derived from not TS5 but TS4.

Figure 3 summarizes the concentration of each substrate at the end of the reaction t = 1×10^{3} at 25 °C from α = 0.05 to 0.95. Here, the line of RNH_3^+ is overlapped HCO_3^- line and is behind. Although it is a small amount, it seems that RNHCOOH and $RNH_2^+COO^-$ are also increasing. On the other hand, it is confirmed that $RNHCOO^-$ has a characteristic peak with a maximum value of 0.5. Regarding CO_2, almost the entire amount is absorbed in all range of α = 0.5 to 0.95, alternatively, residual CO_2 increases and the absorption rate deteriorates as α increases.

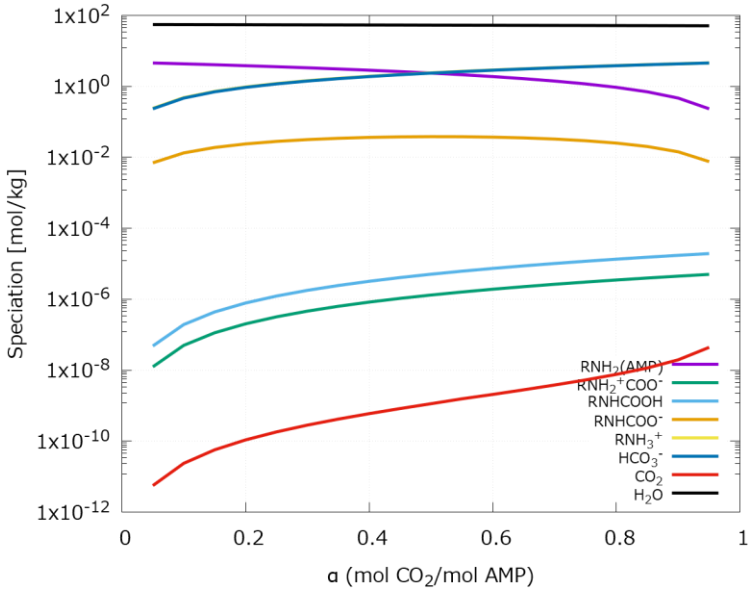

Figure 3 Summarized concentration changes along CO_2 loading at 25 °C.

The probability of computational prediction can be confirmed by comparing it with the actual measurement. Ciftja *et al.* [7] have measured precise product concentrations using NMR for the reaction. Figure 4 plots the measured values by Ciftja *et al.* and our values calculated by Kinerator for each CO_2 loading at 25 °C. In this system, according to the thermodynamic control, it is expected that bicarbonate (HCO_3^-) is produced more than carbamate ($RNHCOO^-$). Alternatively, according to the kinetic control, carbamate predominates. Our simulation results for the concentration of AMP, its ammonium ion and HCO_3^- have very good agreement with actual measured values. In contrast, for $RNHCOO^-$, simulated values are lower than actual values. We consider that this is because the free energy of $RNHCOO^- + RNH_3^+$ has been calculated slightly higher than actual one. Assuming that this system follows Boltzmann distribution, the energy difference to produce 10 times difference of concentration ratio at room temperature is calculated to be 1.4 kcal mol^{-1}. Therefore, if $RNHCOO^- + RNH_3^+$ could be stabilized by this value of energy, the production ratio of $RNHCOO^-$ is anticipated to increase. On the contrary, in this case, $HCO_3^- + RNH_3^+$ is stabilized due to breaking the above thermodynamic control and the concentration of HCO_3^- will be lower than that of $RNHCOO^-$. Like this, kinetic simulation results are enormously influenced by estimated energies by theoretical calculations. Hence, in order to obtain accurate absolute values by kinetic simulations, it is a prerequisite that free energies of reactions, especially energy differences between transition states and stable substrates.

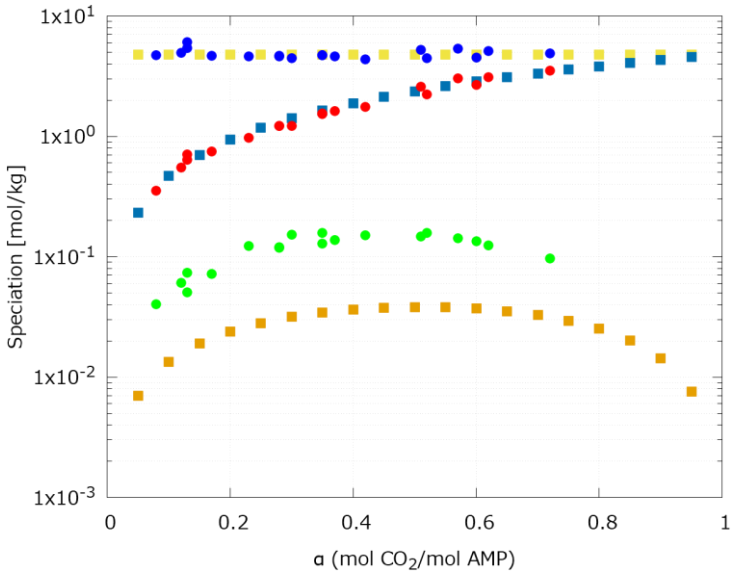

Figure 4 Comparisons between simulated and actual measurement concentrations at 25 °C.

4. Conclusion

In this study, we showed the considerable formula for the reaction kinetics for the complex systems. We applied Kinerator adopted this formula to CO_2 absorption reaction by AMP and clarify the time differential change of the reaction profile and the dependence of CO_2 concentrations. Our results reproduced actual measurement values with extremely high accuracy. The application in this time is for the homogenous system in standard condition. In our future study, we will extend it to practical conditions such as heterogeneous, open and other systems with applying the entropy term, the temperature increasing term by the exothermic enthalpy, the diffusion coefficient of gas and so on.

Acknowledgement

The part of this study is based on results obtained from a project, JPNP14004, commissioned by the New Energy and Industrial Technology Development Organization (NEDO).

References

[1] H. Eyring, M. Polanyi, Z. Phys. Chem. 12 (1931) 279
[2] H. Eyring, J. Chem. Phys. 3 (1935) 107–115
[3] M. G. Evans, M. Polanyi, Trans. Faraday Soc. 31 (1935) 875
[4] K. J. Laidler, M. C. King, J. Phys. Chem. 87 (1983) 2657–2664

[5] K. J. Laidler, The Chemical Intelligencer 4 (1998) 39–47
[6] T. Yamaguchi, H. Yamada, K. Hori, KAGAKU KOGAKU RONBUNSHU 43 (2017) 111–116
[7] A. F. Ciftja, A. Hartono, E. F. da Silva, H.F. Svendsen, Energy Procedia 4 (2011) 614–620
[8] H. Yamada, Y. Matsuzaki, T. Higashii, S. Kazama, J. Phys. Chem. A 115 (2011) 3079–3086
[9] A. V. Marenich, C. J. Cramer, D. G. Truhlar, J. Phys. Chem. B 113 (2009) 6378–6396
[10] Gaussian 09, Revision A.02, M. J. Frisch, G. W. Trucks, H. B. Schlegel, G. E. Scuseria, M. A. Robb, J. R. Cheeseman, G. Scalmani, V. Barone, G. A. Petersson, H. Nakatsuji, X. Li, M. Caricato, A. Marenich, J. Bloino, B. G. Janesko, R. Gomperts, B. Mennucci, H. P. Hratchian, J. V. Ortiz, A. F. Izmaylov, J. L. Sonnenberg, D. Williams-Young, F. Ding, F. Lipparini, F. Egidi, J. Goings, B. Peng, A. Petrone, T. Henderson, D. Ranasinghe, V. G. Zakrzewski, J. Gao, N. Rega, G. Zheng, W. Liang, M. Hada, M. Ehara, K. Toyota, R. Fukuda, J. Hasegawa, M. Ishida, T. Nakajima, Y. Honda, O. Kitao, H. Nakai, T. Vreven, K. Throssell, J. A. Montgomery, Jr., J. E. Peralta, F. Ogliaro, M. Bearpark, J. J. Heyd, E. Brothers, K. N. Kudin, V. N. Staroverov, T. Keith, R. Kobayashi, J. Normand, K. Raghavachari, A. Rendell, J. C. Burant, S. S. Iyengar, J. Tomasi, M. Cossi, J. M. Millam, M. Klene, C. Adamo, R. Cammi, J. W. Ochterski, R. L. Martin, K. Morokuma, O. Farkas, J. B. Foresman, and D. J. Fox, Gaussian, Inc., Wallingford CT, (2016)